Tohoku J. Exp. Med., 2023, **260**, 149-163

Ferulic Acid Alleviates Hepatic Lipid Accumulation and Inflammation by Improving Proximal and Distal Intestinal Barriers in NAFLD Mice

Jiaojiao Fu,[1,2,*] Jingyan Yang,[1,2,*] Liying He,[3] Caixia Yang,[3] Jing He,[1,2] Yanan Hua,[1,2] Jinlin Guo[1,2,3] and Sijing Liu[1,2]

[1]College of Medical Technology, Chengdu University of Traditional Chinese Medicine, Chengdu, Sichuan, China
[2]Chongqing Key Laboratory of Sichuan-Chongqing Co-construction for Diagnosis and Treatment of Infectious Diseases Integrated Traditional Chinese and Western Medicine, Chengdu, Sichuan, China
[3]Key Laboratory of Characteristic Chinese Medicine Resources in Southwest China, College of Pharmacy, Chengdu University of Traditional Chinese Medicine, Chengdu, Sichuan, China

Non-alcoholic fatty liver disease (NAFLD) is closely associated with low-grade chronic inflammation which is usually induced by intestinal dysbiosis. As ferulic acid (FA) has been proven effective at improving the intestinal integrity, we aimed to determine the effect of dietary FA on NAFLD development in high-fat dieted (HFD) mice, a well-established model of NAFLD. Male C57BL/6J mice were fed either a normal chow diet (ND) or HFD with or without FA (40 mg/kg) orally for 6 weeks. FA significantly alleviated lipid metabolism disorder and reduced liver inflammation in HFD mice ($P < 0.05$). As expected, FA improved the ileal intestinal integrity likely via the Nuclear factor E2-related factor 2 (Nrf2)/Heme oxygenase-1 (HO-1) signaling pathway. Importantly, we found that FA also relieved HFD-induced gut microbiota dysbiosis by inhibiting the growth of harmful bacteria such as *Helicobacter* and increased the abundance of many short-chain fatty acids (SCFAs)-producing bacteria ($P < 0.05$). Our data indicated that FA not only increased the colonic levels of SCFAs, but also maintained the colonic barrier integrity by up-regulating the expression of the epithelial tight junction protein. These data indicated that FA alleviated NAFLD by reducing circulating lipopolysaccharide levels. These effects may be due to improved proximal and distal intestinal barriers, which presumably mediated through the interaction of FA with the gut microbiota.

Keywords: ferulic acid; gut microbiota-liver axis; intestinal barrier; non-alcoholic fatty liver disease; short chain fatty acid
Tohoku J. Exp. Med., 2023 June, **260** (2), 149-163.
doi: 10.1620/tjem.2023.J023

Introduction

Non-alcoholic fatty liver disease (NAFLD) has recently become the most prevalent chronic liver disease, affecting a quarter of the world's population (Tilg et al. 2020, 2021). NAFLD includes a wide range of manifestations characterized by hepatic lipid accumulation, inflammation, and fibrosis (Tilg et al. 2021). Left untreated, NAFLD usually progresses to cirrhosis and liver cancer (Tilg et al. 2021). Currently, lipid-lowering drugs, such as metformin and statins, are still the most common treatments for NAFLD. However, these drugs exhibit many side effects, including gastrointestinal disorders, hepatotoxicity, and muscle pain (Singh et al. 2017). Therefore, additional strategies that alleviate NAFLD with fewer side effects are still required. The pathogenesis of NAFLD is complex and incompletely understood, but a growing body of research suggest that the development of NAFLD is closely related to the gut-liver axis disorder (Tilg et al. 2020; Wang et al. 2022a). According to the most accepted theory, the multi-

Received January 19, 2023; revised and accepted March 7, 2023; J-STAGE Advance online publication March 16, 2023
*These two authors contributed equally to this work.
Correspondence: Sijing Liu, College of Medical Technology, Chengdu University of Traditional Chinese Medicine, No.1166, Liutai Dadao, Wenjiang District, Chengdu, Sichuan 610075, China.
e-mail: liusijing@cdutcm.edu.cn
Jinlin Guo, College of Medical Technology, Chengdu University of Traditional Chinese Medicine, No.1166, Liutai Dadao, Wenjiang District, Chengdu, Sichuan 610075, China.
e-mail: guo596@cdutcm.edu.cn

ple 'gastrointestinal hits' hypothesis, the progression of NAFLD is initiated by disruption of the microbiota and intestinal barrier dysfunction (Tilg et al. 2020; Wang et al. 2022a). These intestinal disorders subsequently lead to the translocation of bacterial metabolites, such as lipopolysaccharide (LPS), which triggers liver inflammation and further aggravates NAFLD through the toll-like receptor 4 (TLR4) signaling pathway (Tilg et al. 2020; An et al. 2022; Wang et al. 2022a). Therefore, efforts to improve gut microbiota and intestinal integrity may be a promising strategy against NAFLD.

At present, no drugs have been approved for the treatment of the impaired intestinal barrier. However, many studies have shown that lifestyle changes, especially dietary supplements, are very effective way to regulate gut microbiota and improve the intestinal barrier (Suzuki 2020; Xie et al. 2020). Ferulic Acid (FA) is a natural phenolic acid that is widely found in natural foods such as cereals, coffee, and berries (Zhao and Moghadasian 2008). It is also an important active component in many traditional Chinese medicines, including *Ligusticum chuanxiong*, *Ranunculaceae*, *Gramineae*, *Angelica*, *Cimicifuga*, *rhizoma spargani*, and so on (Li et al. 2021a). Similar to other polyphenolic compounds, FA has free radical scavenging effects *in vitro* and *in vivo*. Recently, several studies suggested that FA was beneficial for NAFLD (Wei et al. 2021; Luo et al. 2022). Additionally, due to its antioxidant capacity, FA has been found to improve the intestinal barrier function in various cellular and animal models (He et al. 2019, 2020; Chen et al. 2022; Hwang et al. 2022; Wan et al. 2022; Wang et al. 2022b). However, FA is known to be rapidly absorbed in the small intestine with a low bioavailability after oral administration (Li et al. 2011). Furthermore, the elimination rate of FA in mice is very fast (Ma et al. 2019). This seems to contradict its powerful biological effects. Recently, researchers have confirmed that some natural products with low bioavailability may act mainly by regulating the gut microbiota (Shin et al. 2014; Chen et al. 2016).

Therefore, we hypothesized that dietary FA supplementation would alleviate NAFLD through interactions with the gut microbiota. In the present study, we set out to determine the effect of dietary FA supplementation on hepatic lipid accumulation and inflammation in the progression of NAFLD and explore the potential mechanisms, using high-fat fed mice.

Materials and Methods

Materials and reagents

Ferulic acid (FA, purity ≥ 98%) was obtained from Dalian Meilun Biotechnology (Dalian, China). Acetic, propionic, butyric, isobutyric, isovaleric, and valeric acid standards were provided by the Sigma-Aldrich Chemical Co., Ltd. (St. Louis, MO, USA). The antibodies of Nrf2 (16396-1-AP), Kelch-like ECH-associated protein 1 (Keap1,10503-2-AP), Heme oxygenase-1(HO-1,10701-1-AP), and Nuclear factor kappa B p65 (NF-κB p65,10745-1-AP) were purchased from Proteintech (Wuhan, China). The antibodies of p38 Mitogen-activated protein kinase (p38 MAPK, A0227), Phospho-p38 MAPK (P-p38, AP0057), Phospho-NF-κB p65 (P-p65, AP0446) were purchased from ABclonal (Wuhan, China). The β-actin antibody (GB11001) was the production of Servicebio (Wuhan, China).

Animal experiments

Forty male C57BL/6 mice (SPF level, 8-week-old) were obtained from Chengdu Dossy Experimental Animals Co., Ltd (Sichuan, China). The study was reviewed by the Ethics Committee of the Affiliated Hospital of Chengdu University of Traditional Chinese Medicine (Ethics No: 2022DL-019). The animals were maintained on a standard 12 h light/dark cycle with a temperature-controlled environment with free access to water. After 7 days of acclimatization, the animals were randomly divided into 4 groups (n = 10 per group) for a 8-week experiment: (1) The normal chow diet group (ND), which was administrated with the chow diet (Supplementary Table S1) and orally administrated with the vehicle (3% tween-80); (2) The high-fat diet group (HFD), which was administered with the high-fat diet (Supplementary Table S1) and the vehicle (3% tween-80); (3) Ferulic acid supplementation group (HFD + FA), which was fed HFD accompanied with FA of 40 mg/kg/day. (4) Positive drugs group (HFD + Statin), which was fed HFD accompanied with lovastatin of 3.3 mg/kg/day. Body weight, water intake, and food consumption were recorded weekly. Mice were fasted overnight before being sacrificed. The samples of blood, liver, spleen, kidney, cecal content, ileum, as well as colon were collected and stored at −80℃ for further analysis.

Biochemical analysis

The serum levels of triglyceride (TG), total cholesterol (TC), alanine aminotransferase (ALT), and alkaline phosphatase (ALP) were measured by the automatic biochemical analyzer (Mindray, Shenzhen, China) with the corresponding kits. Serum lipopolysaccharide (LPS) concentrations were determined using a chromogenic Limulus amebocyte lysate endotoxin assay kit (ToxinSensor, GenScript, Piscataway, NJ, USA) according to the manufacturer's instructions.

Histopathological analysis

The liver and small intestine samples were fixed in 4% paraformaldehyde, embedded, and sectioned. The sections of liver and small intestine were stained with hematoxylin-eosin (HE) according to a standard procedure. The sections of liver were also stained with Oil Red O.

Measurement of total superoxide dismutase (T-SOD) level

The superoxide dismutase (SOD) content was determined with assay kits, which purchased from Elabscience

Bioengineering Institute of Wuhan (Wuhan, China) according to the manufacturer's protocols.

Immunofluorescence staining

Unstained paraffin sections were deparaffinized in xylenes and washed for three times, then rehydrated in decreasing ethanol concentrations (100%, 85%, 75%, and 0%). Antigen retrieval was achieved by boiling in EDTA antigen retrieval buffer. After autofluorescence quenching, the sections were blocked with 5% goat serum solution, subsequently incubated with antibodies of Zona occludens 1 (ZO-1), Claudin-1, and Occludin (1:500 dilution; Servicebio) overnight at 4℃. The samples were then washed, incubated with an appropriate secondary antibody (1:300 dilution; Servicebio) and counterstained with 4',6-diamidino-2-phenylindole (DAPI) for the staining of nucleus. The immunofluorescent images were observed under a fluorescence microscope (Nikon, Tokyo, Japan) and images were collected.

Quantitative real time-PCR (qRT-PCR) analysis

Total RNA samples of tissues and cells were obtained by RNA-easy isolation reagent (Vazyme, Nanjing, China) and then were reverse transcribed into cDNA. The cDNA was generated from 1 μg RNA using the Evo M-MLV RT mix kit with gDNA clean (Accurate Biotechnology, Hunan, China). QRT-PCR was then performed utilizing SYBR® Green Premix Pro Taq reagent kit (Accurate Biotechnology) on the Real-Time PCR System (Jena, Germany) for 40 cycles (95°C for 30 s, 95°C for 5 s, and 60°C for 30 s). The expression levels of target gene were calculated by $2^{-\Delta\Delta Ct}$ method with GAPDH selected as internal reference. The specificity of all PCR products was checked using melting curve analysis. The sequences of quantitative real-time PCR primers used in this study are shown in Supplementary Table S2.

Western blot analysis

Tissue samples were homogenized in cold RIPA lysis buffer (Boster, Wuhan, China) with protease and phosphatase inhibitors on the ice for 30 min. After centrifugation (12,000 × *g*, 10 min, 4°C), the supernatants were then collected. BCA protein assay kit (Beyotime, Jiangsu, China) was used to quantify protein levels of the supernatants. Total protein from tissue in the lysate was separated by 10% SDS-PAGE gels and then transferred onto a polyvinylidene fluoride (PVDF) membrane (Millipore, Burlington, MA, USA). The membrane was blocked with 5% non-fat milk in Tris Buffered Saline with Tween®20 (TBS-T) buffer for 1 h at room temperature and then the membranes were incubated with primary antibodies against p38 MAPK (1:500), Phospho-p38 MAPK (1:500), Phospho-NF-κB p65 (1:500), NF-κB p65 (1:1,500), Nrf2 (1:500), Keap1 (1:500), HO-1 (1:500) and β-actin (1:1,000) overnight at 4°C. After washing with TBS-T for five times, these membranes were incubated with a corresponding secondary antibody (1:1,000) for 1 h at room temperature. After being washed 5 times of TBS-T, protein bands were finally visualized using an enhanced chemiluminescence detection system (Bio-Rad Laboratories, Hercules, CA, USA). Image J software was used to quantify the immunoblots.

Molecular docking for FA and Keap1

The structure of FA was obtained from PubChem, and the X-ray structure of Keap1 was selected from Protein Data Bank (PDB code: 2Z32). Maestro was used to predict the binding mode of FA with Keap1. The docking workflow followed the 'induced fit' protocol, which allows the side chains of the receptor pocket to move according to the ligand conformations, with a constraint on their positions.

Determination of colonic short-chain fatty acids (SCFAs)

Acetonitrile (100 μL) containing 125 μg/mL internal standard (2-ethylbutyric acid) was added to 50 mg of cecal contents and 50 μL 15% phosphoric acid. Another 1.0 mL acetonitrile was added to the mixture, which was then homogenized and centrifuged at 12,000 × *g* at 4°C for 15 min. Supernatants were filtered with a 0.22 μm filter membrane and analyzed by GC-FID (Agilent Technologies, Santa Clara, CA, USA). SCFAs were separated using the nitroterephthalic acid modified polyethyleneglycol (PEG) column (DB-FFAP, 30 m × 0.53 mm × 1.0 μm; Agilent Technologies). The GC injector was maintained at 240°C. The oven temperature was initially set at 50°C for 1 min, programmed at a rate of 20°C/min to 180°C which was held for 1 min and then at 20°C/min to 200°C that was held for 2 min. The carrier gas was nitrogen at a flow rate of 6.44 mL/min.

Gut microbiota analysis

The total DNA of cecum contents was extracted and the 16S rRNA sequences of bacteria were amplified by PCR using specific primers for V3-V4 regions (forward primer, 5'-TACGGRAGGCAGCAG-3' and the reverse primer, 5'-AGGGTATCTAATCCT-3'). Heatmap and taxon relative abundance bar diagram were created by using custom R scripts and ggplot2.

Preparation of supernatant from colonic contents

The supernatant from colonic contents (SCC) was collected as described previously with modifications (Jing et al. 2021). In brief, the colonic contents were suspended with DMEM medium supplemented with 10% FBS (100 mg/mL). Then, the SCC was obtained by centrifugation at 3,000 ×*g* at 4℃ for 10 min. After that, the SCC was filtered through a 0.22 μm filter and diluted (1:10) with DMEM-10% FBS medium and used for co-incubation studies.

Cell culture and co-incubation

Caco-2, a human colon adenocarcinoma cell line acquired from Stem Cell Bank, Chinese Academy of Sciences (Shanghai, China), was maintained in complete

Dulbecco modified Eagle medium (DMEM) with 10% fetal bovine serum (FBS), penicillin (100 U/mL) and streptomycin (100 μg/mL) as well as 1% nonessential amino acids, and was kept at a controlled temperature of 37°C with 5% CO_2 atmosphere. Caco-2 cells were seeded in 6-well plates (1×10^6 cells/well) and incubated for 24 h. Then, cells were treated with SCC of colonic contents collected from ND, HFD and HFD + FA groups for 48 h. Cells were then rinsed and scraped for q-PCR analysis.

Statistical analysis

Experiments were conducted separately at least three times, and the data were expressed as means ± standard deviation (SD). All Statistical analysis was performed using GraphPad Prism8.0 (GraphPad Software, La Jolla, CA, USA). The analysis of variance (ANOVA) followed by Dunnett-*t* test was used for multiple-comparison between groups, while Student's *t*-test was performed to evaluate differences between two groups. $P < 0.05$ was considered to indicate a statistically significant difference.

Results

FA administration prevented lipid metabolism disorder in HFD-fed mice.

To investigate the beneficial effects of FA, 8 weeks old C57BL/6J mice were fed a high-fat diet (HFD) with or without FA supplementation for 8 weeks (Fig. 1A). We found that daily oral administration of FA had no significant effect on body weight as well as the serum TC concentrations during the 8 weeks (Fig. 1B-D). Concomitantly, FA did not affect the liver index, spleen index, kidney index, serum ALT and AST concentrations of these mice (Supplementary Fig. S1). However, the serum TG levels were significantly reduced in FA-treated mice ($P < 0.05$, Fig. 1E), and it was not related to the changes in the food intake (Fig. 1F). Interestingly, these findings may be associated with the increased water consumption after FA intervention ($P < 0.01$, Fig. 1G). In line with the decreased serum TG concentrations, FA attenuated the ballooning degeneration of liver cells and decreased hepatic lipid accumulation in mice, compared to those of the HFD group, as assessed by HE and oil red staining ($P < 0.01$, Fig. 1H, I). Taken together, these results indicated that FA supplementation could significantly improve lipid metabolism disorder in high-fat diet-induced mice. But it is interesting that FA supplementation significantly reduced hepatic *Fasn* mRNA expression without affecting *Hmg-cr* mRNA levels (Supplementary Fig. S2), suggesting that FA improved lipid metabolism disorder by a different mechanism than statins.

FA alleviated hepatic inflammation in HFD-fed mice

To evaluate the effect of FA on liver inflammation induced by high-fat diet, we further analyzed the relative mRNA expression of inflammation cytokines, including *Il-1β*, *Il-6*, and *Tnf-α*, in livers. As expected, the expression levels of *Il-1β*, *Il-6*, and *Tnf-α* were higher in the liver tissues of HFD mice than those of the ND group ($P < 0.05$, Fig. 2A-C). Meanwhile, the levels of *Il-6* were slightly, yet not significantly, reduced in FA-treated mice (Fig. 2B), whereas the diet-induced high expression of *Il-1β* and *Tnf-α* were fully altered by FA treatment ($P < 0.01$, Fig. 2A-C). However, statin intervention did not affect the expression levels of inflammatory cytokines (Fig. 2A-C), which further demonstrated that FA improved NAFLD by a different mechanism from statins. As circulating lipopolysaccharide (LPS) is known to cause a range of liver-related inflammatory responses, we determined the effect of FA on serum LPS levels. As shown in Fig. 2D, higher serum LPS levels were detected in the HFD mice ($P < 0.0001$), while these levels were significantly decreased after the treatment of FA ($P < 0.05$). Consistent with the reduced circulating LPS levels, FA-treated mice showed lower expression of *Tlr4* and *Myd88* in the liver tissues than those in HFD mice ($P < 0.05$, Fig. 2E, F). These results implied that the reduction in hepatic inflammatory responses after FA supplementation was probably due to the LPS-lowering effect of FA.

FA improved the ileal intestinal barrier and induces the ileal Nfr2/HO-1 signaling pathway

Considering that FA is absorbed mainly in the small intestine and the integrity of the intestinal barrier plays a key role in the serum LPS content (Li et al. 2011), we first assessed whether FA affected the structure and function of the ileum. As illustrated by representative images in Fig. 3A and B, the ileal tissue of HFD-fed mice showed a reduced length of gut villi ($P < 0.05$) and damaged intestinal integrity, whereas these changes were significantly improved by FA treatment ($P < 0.05$). We also found that FA intervention markedly increased the mRNA and protein expressions of ZO-1 and Occludin in the ileum ($P < 0.05$, Fig. 3C-H). Although the protein expression of Claudin-1 was slightly, but not significantly increased in HFD + FA group (Fig. 3I, J), its mRNA expression level was greatly increased after FA supplementation ($P < 0.05$, Fig. 3K). These findings demonstrated that FA might protect the ileal barrier by up-regulating epithelial tight junction proteins. In addition, we further measured the levels of pro-inflammatory cytokines and SOD in ileum. The ileal *Il-1β*, *Il-6*, and *Tnf-α* levels were not different between the groups (Supplementary Fig. S3), but the SOD levels in the ileum were significantly increased after FA supplementation ($P < 0.001$, Fig. 4A). Furthermore, the ileal nuclear factor-erythroid 2-related factor 2 (Nrf2) and heme oxygenase 1 (HO-1) were significantly up-regulated at both mRNA and protein levels ($P < 0.05$, Fig. 4B-F, original image in Supplementary Fig. S4). However, FA did not affect the expression of Kelch-like ECH-associated protein 1 (Keap1), the gene upstream of Nrf2 (Fig. 4F, G, Supplementary Fig. S4). Therefore, we speculated that the upregulation of NRF2 was likely the result of FA disrupting the Keap1-NRF2 interaction. This was further supported by the molecular docking analysis. As shown in Fig. 4H and I, FA

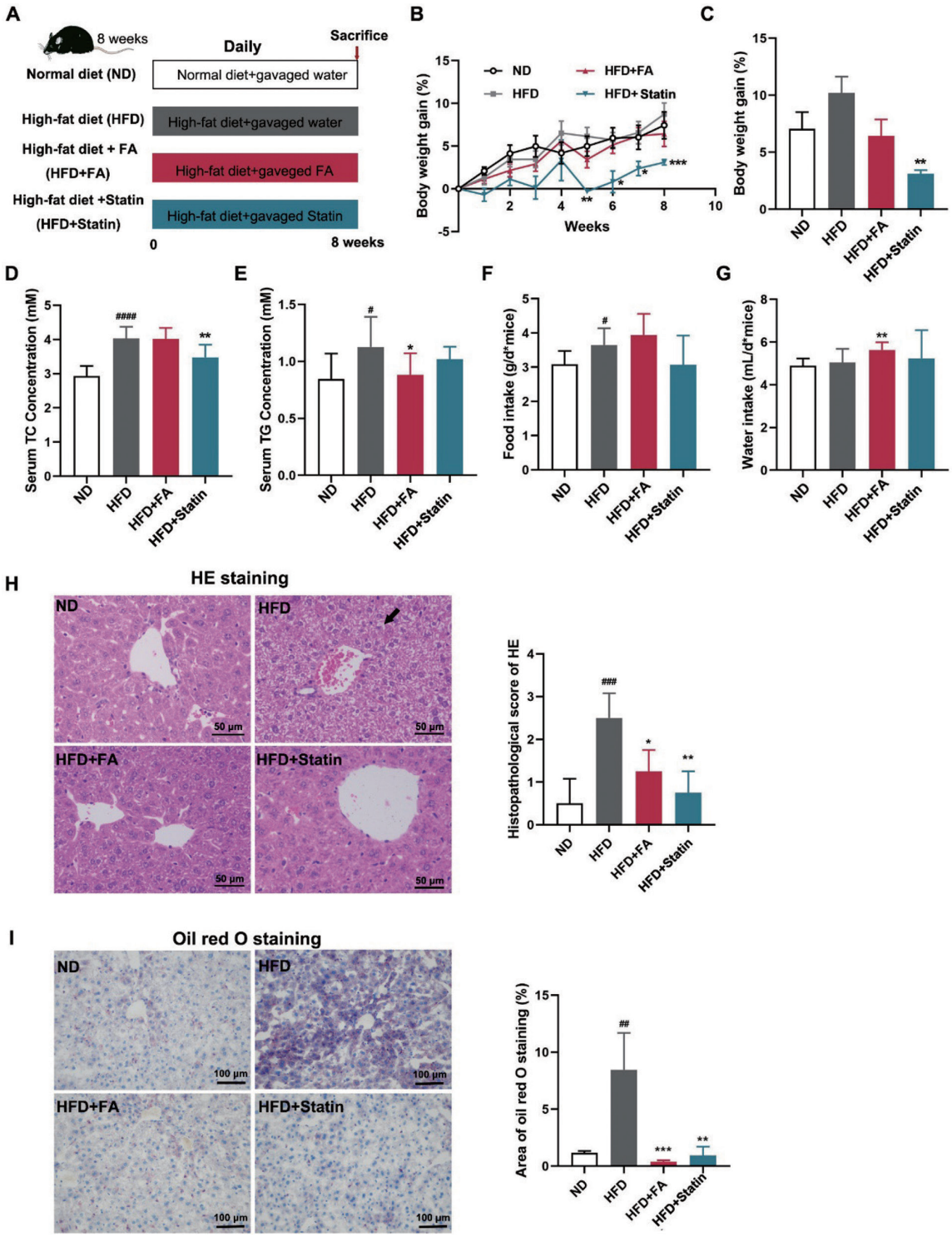

Fig. 1. Ferulic Acid (FA) administration prevented lipid metabolism disorder in high-fat diet (HFD)-fed mice.
(A) Schema showing the animal groups and treatments. Male C56BL/6J mice (n = 10 per group) were fed either a normal chow diet (ND) or a high-fat diet (HFD) and treated with daily doses of sterile water, FA, and rosuvastatin throughout 8 weeks. (B and C) Body weight gain. (D) Serum total cholesterol (TC) concentrations. (E) Serum triglyceride (TG) concentrations. (F) Food intake. (G) Water intake. (H) Representative photographs of the liver sections with hematoxylin-eosin staining (HE). Scale bar, 50 μm. × 400 magnification. An arrow indicates the ballooming degeneration of liver cell. (I) Representative photographs of the liver sections with oil red O staining. Scale bar, 100 μm. × 200 magnification. Data were presented as mean ± SD (n = 10). Multiple groups were tested by one-way ANOVA followed by Dunnett-t test for all statistical analyses. $^{\#}P < 0.05$; $^{\#\#\#\#}P < 0.0001$ (vs. ND group); $^{*}P < 0.05$; $^{**}P < 0.01$ (vs. HFD group).

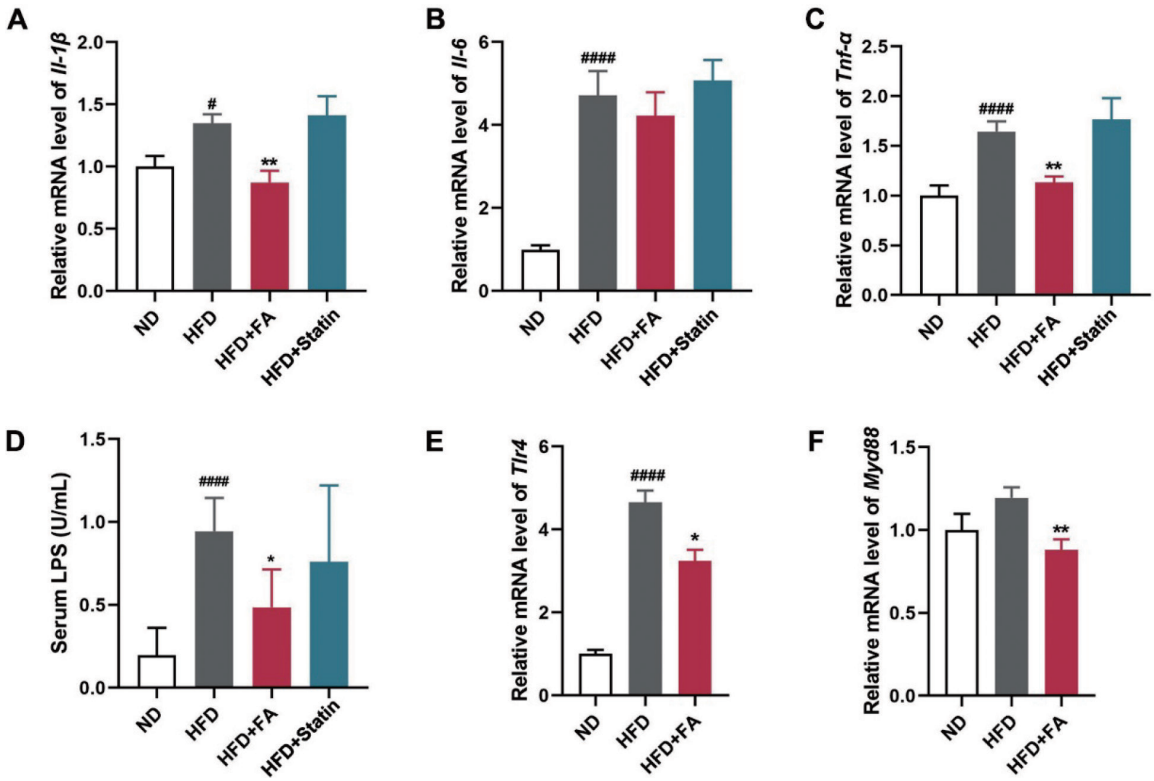

Fig. 2. Ferulic Acid (FA) alleviated hepatic inflammation in high-fat diet (HFD)-fed mice. (A-C) Relative mRNA expression of *Il-1β* (A), *Il-6* (B), and *Tnf-α* (C) in the liver. (D) Serum LPS levels. These results indicated that FA improved non-alcoholic fatty liver disease (NAFLD) by a different mechanism from statins, which is the positive control drug in this study. (E and F) Relative mRNA expression of *Tlr4* (E) and *Myd88* (F) in the liver. Data were presented as mean ± SD (n = 10). Multiple groups were tested by one-way ANOVA followed by Dunnett-t test for all statistical analyses. $^{\#}P < 0.05$; $^{\#\#\#\#}P < 0.0001$ (vs. ND group); $^{*}P < 0.05$; $^{**}P < 0.01$ (vs. HFD group).

may disrupt the Keap1-Nrf2 interaction by binding to the Nrf2-binding pocket of Keap1, as FA may form hydrogen bonds with residue Ile559 and ARG415 of Keap1. These results indicated that FA ameliorated the intestinal barrier in ileum likely by activating Nrf2/HO-1 signaling pathway.

FA administration remodeled the gut microbial communities in HFD-fed mice

The gut-liver axis disorder, particularly dysbiosis of gut microbiota is thought to be a major source of circulating LPS (Tilg et al. 2020; Wang et al. 2022a). To decipher the effects of FA on gut microbiota, we analyzed the changes of the cecal gut microbiota composition and the relative abundance of specific microbial taxa by 16S rRNA gene sequencing. No significant differences were observed in the Shannon index, Chao1 index, and Simpson index (Fig. 5A-C), which indicated that the alpha diversity did not change after FA supplementation. However, the principal component analysis (PCA), a crucial index of *β*-diversity, showed that 8 weeks of FA administration dramatically changed gut microbial profile (Fig. 5D, $P < 0.01$). Additionally, analysis of the gut microbiota at various taxonomic levels demonstrated that FA altered the bacterial composition at phylum level. FA decreased the abundance of Deferribacterota and Campilobacterota, and increased the abundance of Proteobacteria ($P < 0.05$, Fig. 5E), even though it did not affect the microbial richness of Firmicutes and Bacteroidetes (Supplementary Fig. S5A, B). We also observed FA treatment slightly decreased the ratio of Firmicutes/Bacteroidetes, a marker of obesity-induced dysbiosis, but the difference between the groups was not significant (Supplementary Fig. S5C). At the genus levels, differences in microbial communities between the HFD mice and the FA-supplemented mice became more apparent ($P < 0.05$, Fig. 5F and Supplementary Fig. S5D). In particular, FA administration significantly increased the relative abundance of the genus *Prevotella*, *[Ruminococcus]_gnavus_group*, *Alloprevotella*, *Faecalibacterium*, and *Terrisporobacter*, which are considered as SCFAs-producing bacteria ($P < 0.05$, Fig 5G). Additionally, FA treatment decreased the relative abundance of the LPS-producing genera, *Helicobacter* ($P < 0.01$, Fig. 5H). To further investigate the potential function of gut microbiota, the Phylogenetic Investigation of Communities by Reconstruction of Unobserved States (PICRUSt) were used to predict the relative abundance of Kyoto Encyclopedia of Genes and Genomes (KEGG) pathways. The PICRUSt results suggested that the 'Bacterial invasion of epithelial cells', 'Toll and Imd signaling pathway', 'Non-alcoholic fatty liver disease (NAFLD)', and 'p53 signaling' pathway in the FA

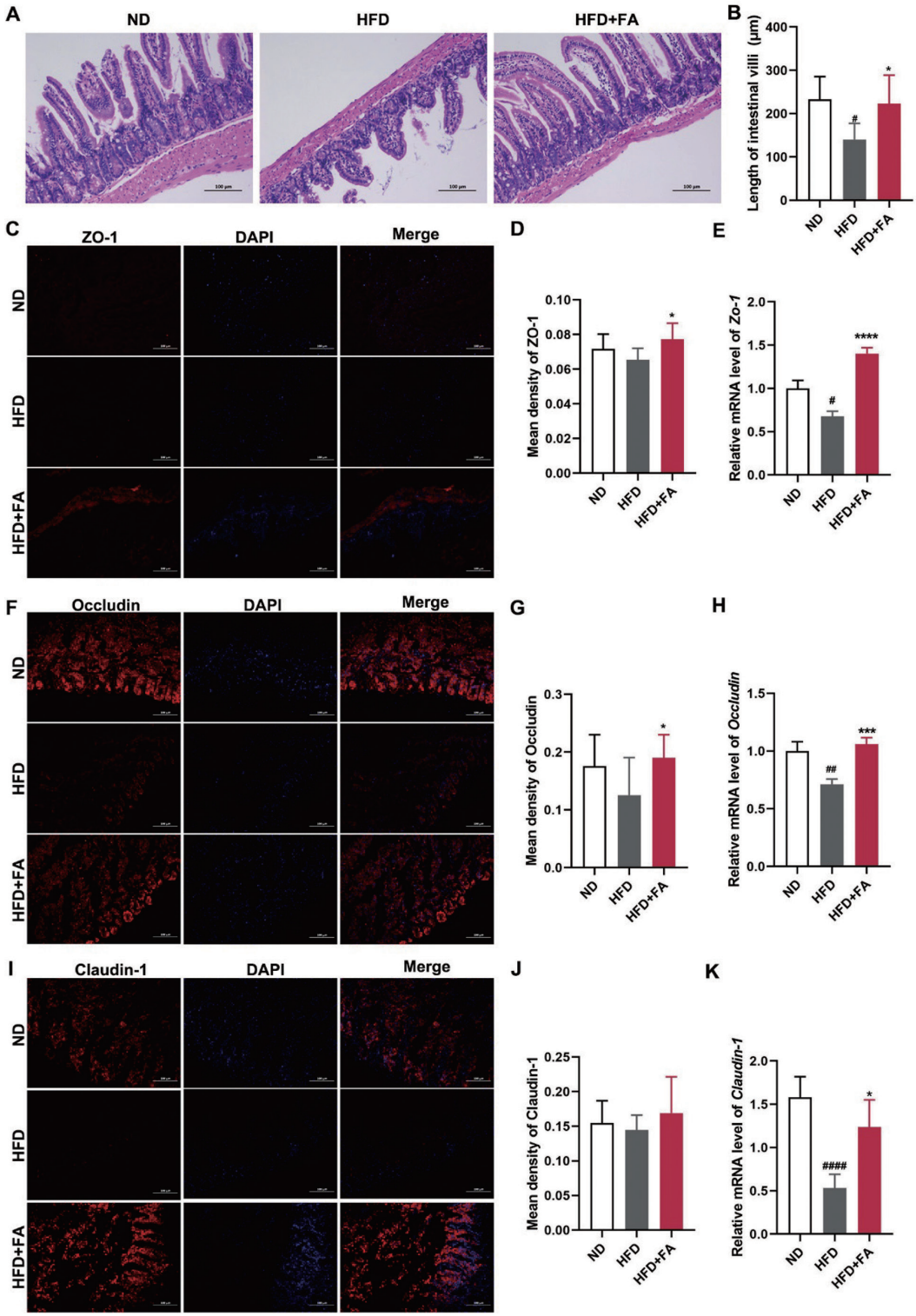

Fig. 3. Ferulic Acid (FA) improved the ileal intestinal barrier in high-fat diet (HFD)-fed mice.
(A) Representative ileal sections with hematoxylin-eosin staining (HE). Scale bar, 100 μm. × 200 magnification. (B) Length of intestinal villi in the ileum. (C and D) Representative immunofluorescence staining of ileal ZO-1 and quantification (n = 5). Scale bar, 100 μm. × 200 magnification. (E) Relative mRNA expression of *Zo-1* in the ileum (n = 10). (F and G) Representative immunofluorescence staining of ileal Occludin and quantification (n = 5). Scale bar, 100 μm. × 200 magnification. (H) Relative mRNA expression of *Occludin* in the ileum (n = 10). (I and J) Representative immunofluorescence staining of ileal Claudin-1 and quantification (n = 5). Scale bar, 200 μm. × 200 magnification. (K) Relative mRNA expression of *Claudin-1* in the ileum (n = 10). Data were presented as mean ± SD. Multiple groups were tested by one-way ANOVA followed by Dunnett-t test for all statistical analyses. $^{\#}P < 0.05$; $^{\#\#}P < 0.01$; $^{\#\#\#\#}P < 0.0001$ (vs. ND group); $^{*}P < 0.05$; $^{***}P < 0.001$; $^{****}P < 0.0001$ (vs. HFD group).

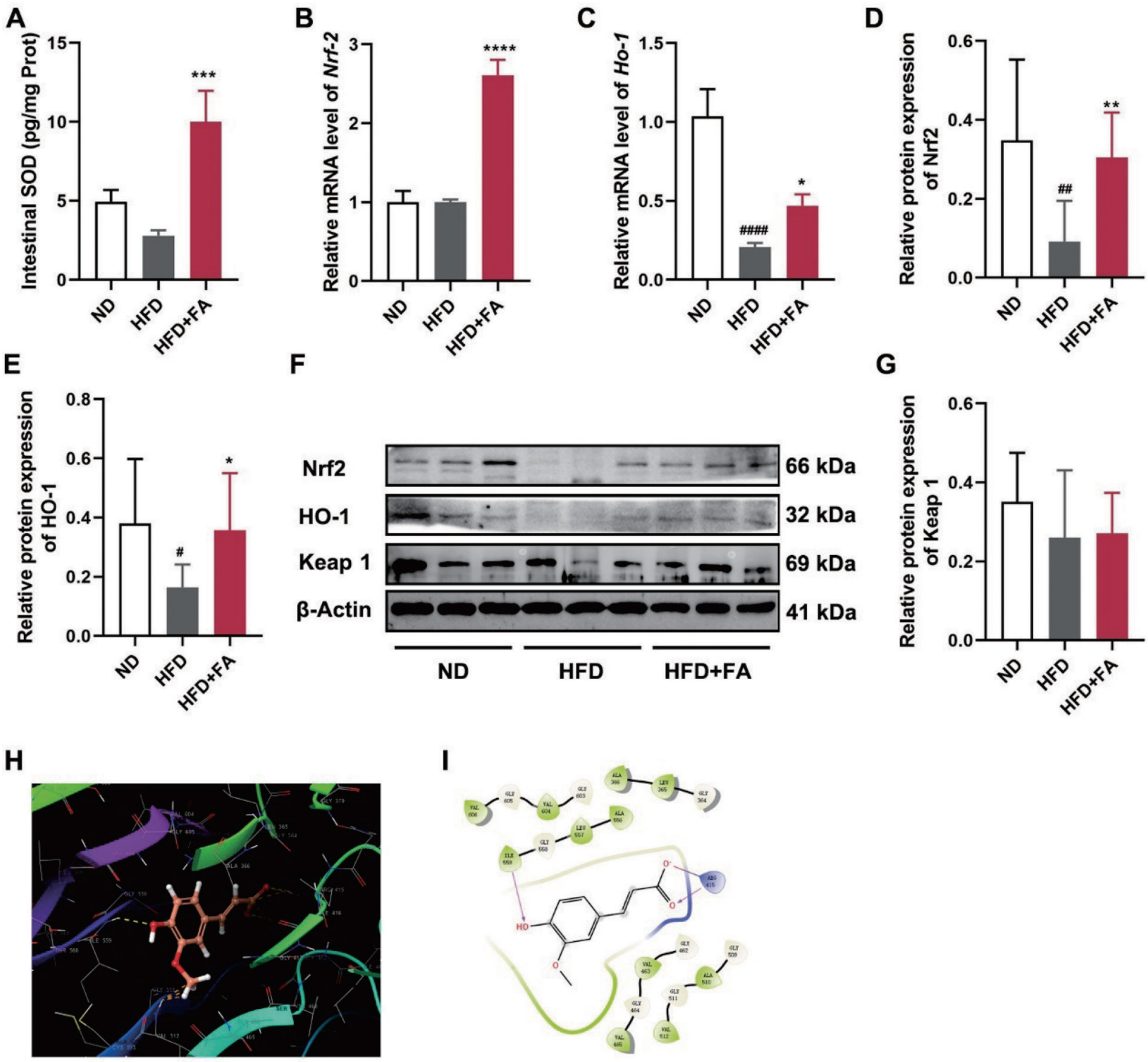

Fig. 4. Ferulic Acid (FA) activated the ileal Nfr2/HO-1 signaling pathway in high-fat diet (HFD)-fed mice.
(A) The ileal superoxide dismutase (SOD) levels. (B and C) Relative mRNA expression of *Nrf2* (B) and *Ho-1* (C) in the ileum. (D-G) Protein levels of Nrf2, HO-1 and Keap1 in the ileum were determined by Western blot. The proposed 3D (H) and 2D (I) binding models of FA with Keap1. The yellow dashed line and the purple arrow represent hydrogen bonds. Data were presented as mean ± SD (n = 10). Multiple groups were tested by one-way ANOVA followed by Dunnett-t test for all statistical analyses. $^{\#}P < 0.05$; $^{\#\#}P < 0.01$; $^{\#\#\#\#}P < 0.0001$ (vs. ND group); $^{*}P < 0.05$; $^{**}P < 0.01$; $^{***}P < 0.001$; $^{****}P < 0.0001$ (vs. HFD group).

group were significantly different compared to those in the HFD group ($P < 0.05$, Fig. 6). Collectively, these data revealed that FA altered the abundance of specific microbial taxa which are closely related to SCFAs and LPS production, and may be involved in maintaining the intestinal barrier integrity.

FA enhanced colonic intestinal barrier, increased the SCFAs concentrations and inhibited the colonic NF-κB and MAPK signaling pathways

Our results have demonstrated that the intestinal barrier integrity may be affected by changes in gut microbiota after FA intervention. Therefore, we determined whether FA supplementation led to differences in the expression of epithelial tight junction proteins. As shown in Fig. 7, FA-fed mice showed up-regulated mRNA levels of *Zo-1*, *Occludin*, and *Claudin-1* in the distal colon as well as protein levels, indicating an increased intestinal integrity aided by FA administration. Furthermore, the relative expression of *Il-1β*, *Il-6* and *Tnf-α* were lower in the colon of FA mice versus HFD control mice ($P < 0.05$, Fig. 8A-C), and these findings were consistent with the decreased *Tlr4* and *Myd88* mRNA levels in the colon of FA mice ($P < 0.001$, Fig. 8D, E). We further assessed bacterial function by analyzing SCFAs in the colonic content of these mice. As we hypothesized, colonic SCFAs levels of mice in the FA group tended to increase, especially acetic acid, butyric acid and total SCFAs levels ($P < 0.05$, Fig. 8F-L). Consistent with dramatically increased SCFAs size, the colonic mRNA expression of *Ffar2* (encodes for GPR43) was up-regulated in FA mice ($P < 0.001$, Fig. 8M). Consistent with the *in vivo* experiments, *in vitro* analysis also showed increased

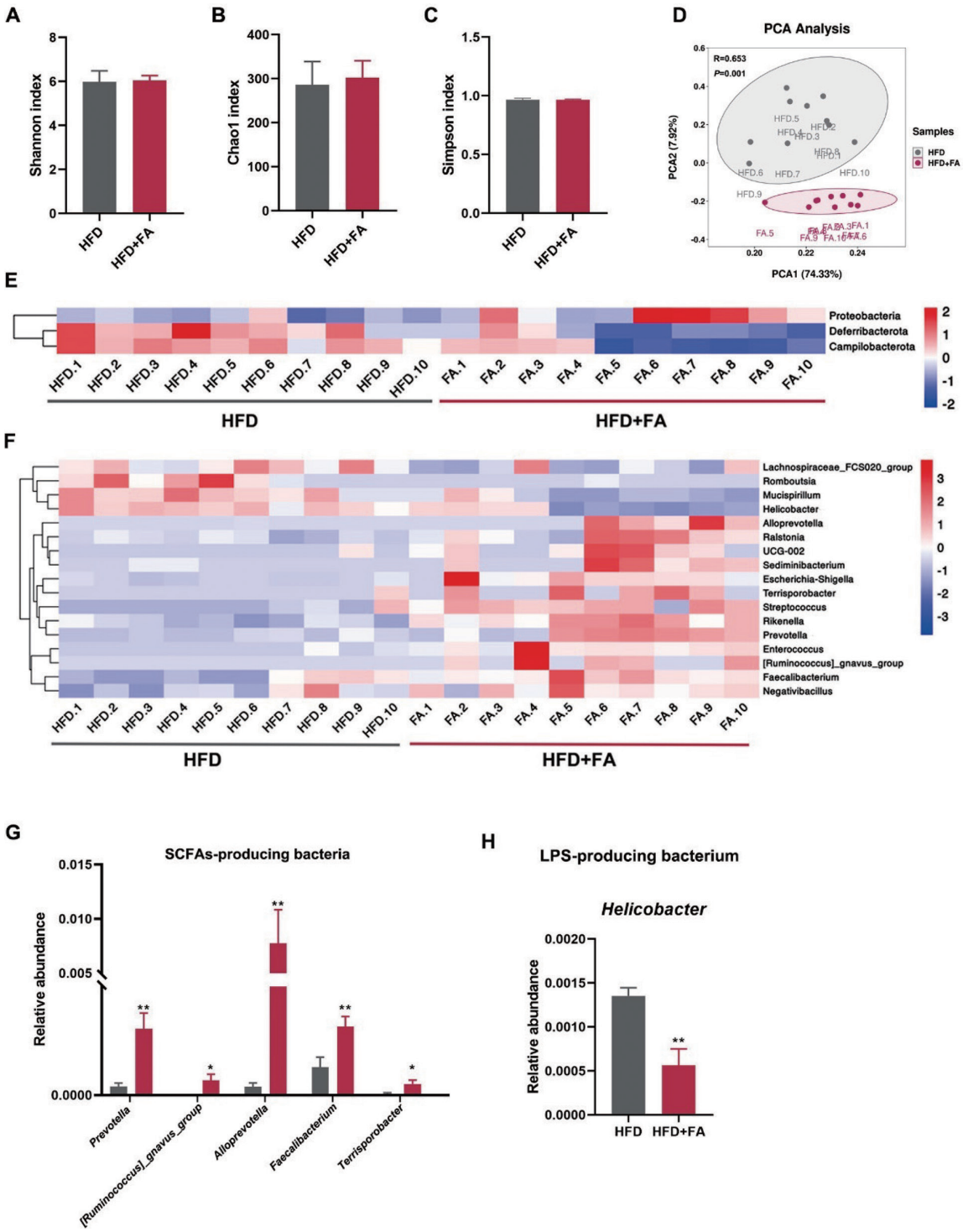

Fig. 5. Ferulic Acid (FA) administration altered the gut microbiota in high-fat diet (HFD)-fed mice.
(A-C) Shannon index (A), Chao1 index (B) and Simpson index (C) at the OUT level. (D) Principal component analysis (PCA) based on unweighted UniFrac distance matrix (at the OTU level). (E and F) Heatmap comparison and hierarchical clustering dendrogram based on the relative abundance of dominant bacteria at the phylum (E) and genus (F) levels. A significance of $P < 0.05$ determined by Student's *t*-test. The relative abundance of each phylum or genus was indicated by a gradient of color from blue to red. (G and H) Relative abundance of the short-chain fatty acid (SCFA)-producing genera (G) and lipopolysaccharide (LPS)-producing genera (H). Data were presented as mean ± SD (n = 10). Differences between two groups were analyzed using the two-tailed Student's *t*-test or the Mann Whitney U test. $^{*}P < 0.05$; $^{**}P < 0.01$ (vs. HFD group).

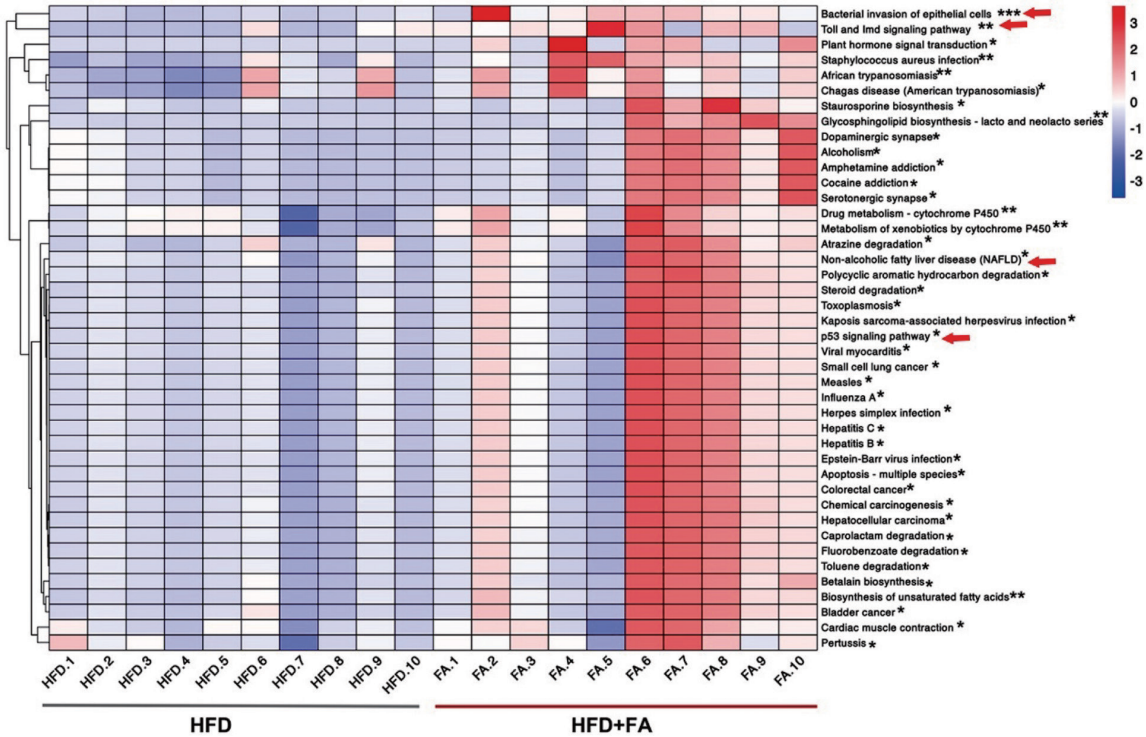

Fig. 6. Predictive functional profiling of microbial communities by the Phylogenetic Investigation of Communities by Reconstruction of Unobserved States (PICRUSt).
The function prediction of microbial genes involved in metabolism by PICRUSt analysis and based on the Welch's t-test. The relative abundance of the Kyoto Encyclopedia of Genes and Genomes (KEGG) pathway at the at L3 level was indicated by a gradient of color from blue to red. $^{*}P < 0.05$; $^{**}P < 0.01$; $^{**}P < 0.001$ (vs. HFD group).

mRNA expressions of *Zo-1*, *Occludin*, *Claudin-5* and *Ffar2* in Caco-2 cells which were treated by cecal content of FA-mice ($P < 0.05$, Fig. 8N-Q). In addition, the ratios of P-p38/p38 and P-p65/p65 in the colon were considerably increased after FA supplementation ($P < 0.05$, Fig. 8R-T, original image in Supplementary Fig. S6). In summary, these data supported that, in addition to improving the small intestinal barrier, FA supplementation could enhance the distal intestinal barrier, and might be involved in the TLR4 and SCFAs-GPR43/NF-κB/MAPK signaling pathways.

Discussion

NAFLD is a huge global burden for which there is few effective treatments (Singh et al. 2017). Recent studies suggest that the development of NAFLD is closely related to the intestinal barrier integrity (Tilg et al. 2020; Wang et al. 2022a). Therefore, changing dietary patterns is an important and cost-effective way to prevent NAFLD. In the present study, we found that FA reduced progression of NAFLD in HFD-fed mice, which was associated with lower hepatic lipid levels and reduced inflammation, possibly by repairing the proximal and distal intestinal barriers and subsequently inhibiting the hepatic Toll-like receptor 4 (TLR4) signaling pathway. In this study, FA administration significantly improved lipid metabolism, especially decreased the hepatic lipid accumulation (Fig. 1), which might be associated with reduced *Fasn* levels (Supplementary Fig. S2). A similar reduction in hepatic fatty acid synthase (FASN) after FA intervention also has been observed in another recent study (Ma et al. 2019). To our knowledge, FASN is a key enzyme involved in hepatic *de novo* lipogenesis, which creates excess TG, and then leads to liver damage in NAFLD (Loomba et al. 2021). Therefore, the inhibitory effect of FA on diet-induced NAFLD might be through reducing the expression of hepatic FASN. However, FA has low bioavailability and is cleared quickly after oral administration (Li et al. 2011). This contradicts its strong biological effect, suggesting that there may be other potential mechanisms.

Notably, in our study, we found that FA supplementation resulted in decreased circulating LPS levels, thereby inhibiting the hepatic TLR4 signaling pathway (Fig. 2). As an important innate immune pattern recognition receptor (PRR), TLR4 has been shown to be up-regulated in patients with NAFLD as well as in animal models, which in turn promotes the progression of hepatic steatosis, inflammation and fibrosis (Hu et al. 2022). It is well-known that TLR4 is normally activated by LPS, which is a major component of the outer membrane of Gram-negative bacteria (Ciesielska et al. 2021). Therefore, it is reasonable to assume that FA might reduce the serum LPS and further alleviate liver inflammation by inhibiting the TLR4 signaling pathway.

It is worth noting that impaired intestinal barrier function and microbial disorders are two important reasons for the increase of circulation LPS. As a protective antioxidant,

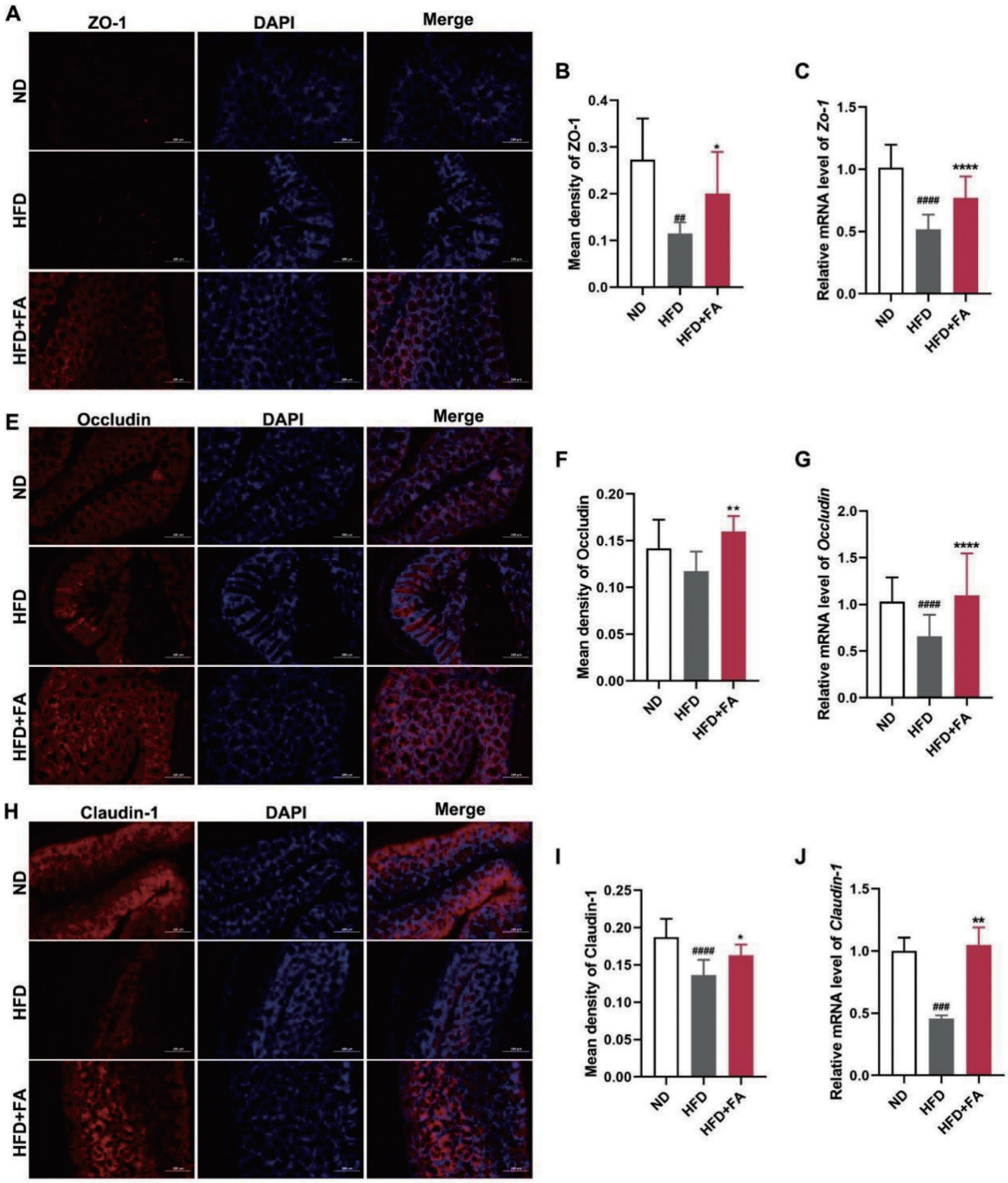

Fig. 7. Ferulic Acid (FA) enhanced colonic barrier function by up-regulating the expression of epithelial tight junction proteins.
(A and B) Representative immunofluorescence staining of colonic ZO-1 and quantification (n = 5). Scale bar, 100 μm. × 200 magnification. (C) Relative mRNA expression of *Zo-1* in the colon (n = 10). (D and E) Representative immunofluorescence staining of colonic Occludin and quantification (n = 5). Scale bar, 100 μm. × 200 magnification. (F) Relative mRNA expression of *Occludin* in the colon (n = 10). (G and H) Representative immunofluorescence staining of colonic Claudin-1 and quantification (n = 5). Scale bar, 100 μm. × 200 magnification. (K) Relative mRNA expression of *Claudin-1* in the colon (n = 10). Data were presented as mean ± SD. Multiple groups were tested by one-way ANOVA followed by Dunnett-t test for all statistical analyses. $^{\#\#}P < 0.01$; $^{\#\#\#}P < 0.001$; $^{\#\#\#\#}P < 0.0001$ (vs. ND group); $^{*}P < 0.05$; $^{**}P < 0.01$; $^{****}P < 0.0001$ (vs. HFD group).

FA has been reported to ameliorate barrier dysfunction in some cell models (He et al. 2016, 2019, 2020; Serreli et al. 2021; Hwang et al. 2022). Considering that FA is absorbed mainly in the small intestine, in this study, we tested the hypothesis that FA could improve the proximal intestinal barrier in HFD-fed mice. As expected, the integrity of the ileum was likely to be enhanced by activating the Nrf2/HO-1 pathway (Figs. 3 and 4). Similar results were also

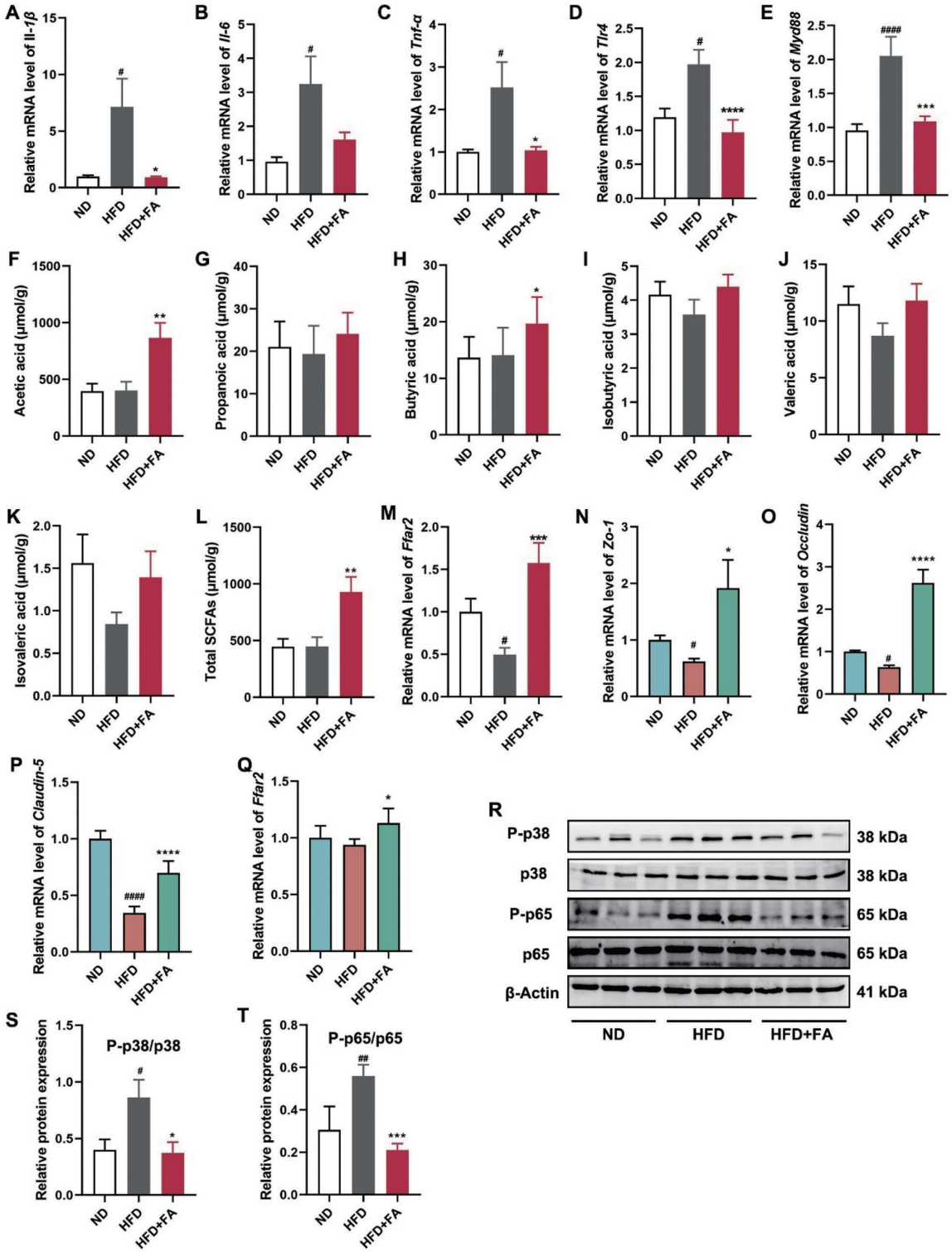

Fig. 8. Ferulic Acid (FA) increased the short-chain fatty acid (SCFA) concentrations in the colon and activated the SCFAs-related signaling pathway.

(A-E) Relative mRNA expression of *Il-1β* (A), *Il-6* (B), *Tnf-α*(C), *Tlr4* (D), and *Myd88* (E) in the colon. (F-L) The concentrations of acetic acid (F), propanoic acid (G), butyric acid (H), isobutyric acid (I), valeric acid (J), isovaleric acid (K), and total SCFAs (L) in colonic contents. (M) Relative mRNA expression of *Ffar2*. (N-Q) Relative mRNA expression of *Zo-1* (N), *Occludin* (O), *Claudin-5*(P), and *Ffar-2*(Q) in Caco-2 cells. (R-T) Protein levels of P-p38, p38, P-p65, and p65 in the colon were determined by Western blot. Data were presented as mean ± SD (n = 10). Multiple groups were tested by one-way ANOVA followed by Dunnett-t test for all statistical analyses. $^{\#}P < 0.05$; $^{\#\#}P < 0.01$; $^{\#\#\#\#}P < 0.0001$ (vs. ND group); $^{*}P < 0.05$; $^{**}P < 0.01$; $^{***}P < 0.001$; $^{****}P < 0.0001$ (vs. HFD group). P-p38, Phospho-p38 MAPK; p38, p38 MAPK; P-65, Phospho-NF-κB p65; p65, NF-κB p65.

observed in other proximal intestines, such as duodenum and jejunum, in other animal models (Chen et al. 2022; Wan et al. 2022; Wang et al. 2022b). However, partially different from previous studies, we found that while FA significantly increased the expression of Nrf2 and its downstream gene *HO-1*, it had no significant effect on its upstream gene *Keap1*. Keap1 is a major negative regulator of NRF2. In cells, Keap1 mediates NRF2 ubiquitination and proteasomal degradation by interacting with NRF2 (Yamamoto et al. 2018). Therefore, decreased Keap1 expression can lead to increased expression of Nrf2 and its downstream genes. Unfortunately, our result was inconsistent with this mechanism. FA did not change the expression of Keap1, the increased expression of Nrf2 was more likely because FA disrupts the binding of Keap1 to Nrf2. To confirm our conjecture, we predicted the binding pattern between FA and Keap1 by molecular docking technique. The results were consistent with our speculation, but the exact relationship still needs to be explored in further studies.

Interestingly, before we started this study, few studies had explored the effects of FA on the distal intestinal barrier and its potential mechanism. However, several studies have reported that FA could modulate the gut microbiota, suggesting that FA may also have the ability to improve the function of the distal intestinal barrier by the interactions with gut microbiota. We therefore evaluated the changes of gut microbiota composition and structure by 16S rRNA gene sequencing. In our study, FA obviously increased the abundance of *Enterococcus*, *Streptococcus*, *Prevotella*, *[Ruminococcus]_gnavus_group*, *Alloprevotella*, *Faecalibacterium*, and *Terrisporobacter*, and dramatically decreased the abundance of *Helicobacter*, *Mucispirillum* and *Romboutsia* (Fig. 5). As a normal commensal, *Enterococcus* was reported to maintain the balance of gut microbiota, and it was positively correlated with almost all barrier function genes (Wu et al. 2021). Similarly, *Streptococcus* has been shown to be negatively correlated with inflammatory cytokines (Wang et al. 2018), which are risk factors for disruption of the intestinal barrier. Additionally, *Prevotella*, *[Ruminococcus]_gnavus_group*, *Alloprevotella*, *Faecalibacterium*, and Terrisporobacter are well-known SCFAs-producing genera (Crost et al. 2013; Ferreira-Halder et al. 2017; Li et al. 2020; Iljazovic et al. 2021; Li et al. 2021b). SCFAs are a major group of bacterial metabolites, mainly including acetate, butyrate, and propionate, are important to maintain intestinal permeability (Liu et al. 2021), indicating that these genera might improve the colonic barrier by increasing the SCFAs levels. On the other hand, *Helicobacter*, a LPS-producing genera, has been evidenced to be positively associated with colonic inflammation (Tian et al. 2021). These results demonstrated that the modulation of gut microbiota might be involved in maintaining the intestinal barrier integrity by the alteration of microbial metabolites, which was consistent with the results of PICRUSt analysis (Fig. 6).

As expected, in this study, we observed that FA enhanced the colonic intestinal barrier function accompanied by increased levels of SCFAs (Figs. 7 and 8), which interestingly supported the findings of a recent study (Tian et al. 2022). Consistent with previous studies, SCFAs could down-regulate the NF-κB and MAPK signaling pathway by activating GPR43 (Wang et al. 2021). GPR43 can be activated by SCFAs, especially acetate, propionate and butyrate. This is in accordance with the increased acetate and butyrate levels in this study (Yamamoto et al. 2018). In addition, previous studies have shown that SCFAs can induce activation of the NF-κB and p38MAPK signaling pathway via GPR43 without significant effects on the other two pathways of MAPK, ERK1/2 and JNK, which is also consistent with our findings (Some results were not shown in this study) (Yonezawa et al. 2007; Yamamoto et al. 2018). This could further explain the underling mechanism by which FA improve the distal intestinal barrier.

In conclusion, the present study demonstrated that FA supplementation effectively alleviated hepatic lipid accumulation and inflammation by modulating the gut microbiota-liver axis, particularly by repairing the proximal and distal intestinal barriers, reducing the circulating LPS levels, and thus inhibiting the hepatic TLR4 signaling pathway. Our results also revealed a novel biochemical mechanism of FA against NAFLD, and thus we can speculate that FA may be a promising natural resource for anti-NAFLD.

Acknowledgments

This work was supported by the National Natural Science Foundation of China (No. 81872959, 81373920, 30801522), the Sichuan Province Youth Innovation Team Fund (No. 19CXTD0055) and the "Xinglin Scholar" Talent Research Promotion Plan of Chengdu University of Traditional Chinese Medicine (grant number 030058032) Science and Technology Department of Sichuan Province (23NSFSC3163).

Conflict of Interest

The authors declare no conflict of interest.

References

An, L., Wirth, U., Koch, D., Schirren, M., Drefs, M., Koliogiannis, D., Niess, H., Andrassy, J., Guba, M., Bazhin, A.V., Werner, J. & Kuhn, F. (2022) The role of gut-derived lipopolysaccharides and the intestinal barrier in fatty liver diseases. *J. Gastrointest. Surg.*, **26**, 671-683.

Chen, M.L., Yi, L., Zhang, Y., Zhou, X., Ran, L., Yang, J., Zhu, J.D., Zhang, Q.Y. & Mi, M.T. (2016) Resveratrol attenuates trimethylamine-N-oxide (TMAO)-induced atherosclerosis by regulating TMAO synthesis and bile acid metabolism via remodeling of the gut microbiota. *mBio*, **7**, e02210-02215.

Chen, X., Wang, Y., Chen, D., Yu, B. & Huang, Z. (2022) Dietary ferulic acid supplementation improves intestinal antioxidant capacity and intestinal barrier function in weaned piglets. *Anim. Biotechnol.*, **33**, 356-361.

Ciesielska, A., Matyjek, M. & Kwiatkowska, K. (2021) TLR4 and CD14 trafficking and its influence on LPS-induced pro-inflammatory signaling. *Cell. Mol. Life Sci.*, **78**, 1233-1261.

Crost, E.H., Tailford, L.E., Le Gall, G., Fons, M., Henrissat, B. & Juge, N. (2013) Utilisation of mucin glycans by the human gut symbiont Ruminococcus gnavus is strain-dependent. *PLoS One*, **8**, e76341.

Ferreira-Halder, C.V., Faria, A.V.S. & Andrade, S.S. (2017) Action and function of Faecalibacterium prausnitzii in health and disease. *Best Pract. Res. Clin. Gastroenterol.*, **31**, 643-648.

He, S., Guo, Y., Zhao, J., Xu, X., Song, J., Wang, N. & Liu, Q. (2019) Ferulic acid protects against heat stress-induced intestinal epithelial barrier dysfunction in IEC-6 cells via the PI3K/Akt-mediated Nrf2/HO-1 signaling pathway. *Int. J. Hyperthermia*, **35**, 112-121.

He, S., Guo, Y., Zhao, J., Xu, X., Wang, N. & Liu, Q. (2020) Ferulic acid ameliorates lipopolysaccharide-induced barrier dysfunction via microRNA-200c-3p-mediated activation of PI3K/AKT pathway in Caco-2 cells. *Front. Pharmacol.*, **11**, 376.

He, S., Liu, F., Xu, L., Yin, P., Li, D., Mei, C., Jiang, L., Ma, Y. & Xu, J. (2016) Protective effects of ferulic acid against heat stress-induced intestinal epithelial barrier dysfunction in vitro and in vivo. *PLoS One*, **11**, e0145236.

Hu, J., Du, H., Yuan, Y., Guo, P., Yang, J., Yin, X., Liu, J., Wu, S., Wan, J. & Gong, X. (2022) MFG-E8 knockout aggravated nonalcoholic steatohepatitis by promoting the activation of TLR4/NF-κB signaling in mice. *Mediators Inflamm.*, **2022**, 5791915.

Hwang, H.J., Lee, S.R., Yoon, J.G., Moon, H.R., Zhang, J., Park, E., Yoon, S.I. & Cho, J.A. (2022) Ferulic acid as a protective antioxidant of human intestinal epithelial cells. *Antioxidants* (*Basel, Switzerland*), **11**, 1448.

Iljazovic, A., Amend, L., Galvez, E.J.C., de Oliveira, R. & Strowig, T. (2021) Modulation of inflammatory responses by gastrointestinal Prevotella spp. - from associations to functional studies. *Int. J. Med. Microbiol.*, **311**, 151472.

Jing, W., Dong, S., Luo, X., Liu, J., Wei, B., Du, W., Yang, L., Luo, H., Wang, Y., Wang, S. & Lu, H. (2021) Berberine improves colitis by triggering AhR activation by microbial tryptophan catabolites. *Pharmacol. Res.*, **164**, 105358.

Li, A.L., Ni, W.W., Zhang, Q.M., Li, Y., Zhang, X., Wu, H.Y., Du, P., Hou, J.C. & Zhang, Y. (2020) Effect of cinnamon essential oil on gut microbiota in the mouse model of dextran sodium sulfate-induced colitis. *Microbiol. Immunol.*, **64**, 23-32.

Li, D., Rui, Y.X., Guo, S.D., Luan, F., Liu, R. & Zeng, N. (2021a) Ferulic acid: a review of its pharmacology, pharmacokinetics and derivatives. *Life Sci.*, **284**, 119921.

Li, H., Shang, Z., Liu, X., Qiao, Y., Wang, K. & Qiao, J. (2021b) Clostridium butyricum alleviates enterotoxigenic Escherichia coli K88-induced oxidative damage through regulating the p62-Keap1-Nrf2 signaling pathway and remodeling the cecal microbial community. *Front. Immunol.*, **12**, 771826.

Li, Y., Liu, C., Zhang, Y., Mi, S. & Wang, N. (2011) Pharmacokinetics of ferulic acid and potential interactions with Honghua and clopidogrel in rats. *J. Ethnopharmacol.*, **137**, 562-567.

Liu, P., Wang, Y., Yang, G., Zhang, Q., Meng, L., Xin, Y. & Jiang, X. (2021) The role of short-chain fatty acids in intestinal barrier function, inflammation, oxidative stress, and colonic carcinogenesis. *Pharmacol. Res.*, **165**, 105420.

Loomba, R., Mohseni, R., Lucas, K.J., Gutierrez, J.A., Perry, R.G., Trotter, J.F., Rahimi, R.S., Harrison, S.A., Ajmera, V., Wayne, J.D., O'Farrell, M., McCulloch, W., Grimmer, K., Rinella, M., Wai-Sun Wong, V., et al. (2021) TVB-2640 (FASN inhibitor) for the treatment of nonalcoholic steatohepatitis: FASCINATE-1, a randomized, placebo-controlled phase 2a trial. *Gastroenterology*, **161**, 1475-1486.

Luo, Z., Li, M., Yang, Q., Zhang, Y., Liu, F., Gong, L., Han, L. & Wang, M. (2022) Ferulic acid prevents nonalcoholic fatty liver disease by promoting fatty acid oxidation and energy expenditure in C57BL/6 mice fed a high-fat diet. *Nutrients*, **14**, 2530.

Ma, Y., Chen, K., Lv, L., Wu, S. & Guo, Z. (2019) Ferulic acid ameliorates nonalcoholic fatty liver disease and modulates the gut microbiota composition in high-fat diet fed ApoE(-/-) mice. *Biomed. Pharmacother.*, **113**, 108753.

Serreli, G., Naitza, M.R., Zodio, S., Leoni, V.P., Spada, M., Melis, M.P., Boronat, A. & Deiana, M. (2021) Ferulic acid metabolites attenuate LPS-induced inflammatory response in enterocyte-like cells. *Nutrients*, **13**, 3152.

Shin, N.R., Lee, J.C., Lee, H.Y., Kim, M.S., Whon, T.W., Lee, M.S. & Bae, J.W. (2014) An increase in the Akkermansia spp. population induced by metformin treatment improves glucose homeostasis in diet-induced obese mice. *Gut*, **63**, 727-735.

Singh, S., Osna, N.A. & Kharbanda, K.K. (2017) Treatment options for alcoholic and non-alcoholic fatty liver disease: a review. *World J. Gastroenterol.*, **23**, 6549-6570.

Suzuki, T. (2020) Regulation of the intestinal barrier by nutrients: the role of tight junctions. *Anim. Sci. J.*, **91**, e13357.

Tian, B., Geng, Y., Wang, P., Cai, M., Neng, J., Hu, J., Xia, D., Cao, W., Yang, K. & Sun, P. (2022) Ferulic acid improves intestinal barrier function through altering gut microbiota composition in high-fat diet-induced mice. *Eur. J. Nutr.*, **61**, 3767-3783.

Tian, B., Zhao, J., Zhang, M., Chen, Z., Ma, Q., Liu, H., Nie, C., Zhang, Z., An, W. & Li, J. (2021) Lycium ruthenicum anthocyanins attenuate high-fat diet-induced colonic barrier dysfunction and inflammation in mice by modulating the gut microbiota. *Mol. Nutr. Food Res.*, **65**, e2000745.

Tilg, H., Adolph, T.E., Dudek, M. & Knolle, P. (2021) Non-alcoholic fatty liver disease: the interplay between metabolism, microbes and immunity. *Nat. Metab.*, **3**, 1596-1607.

Tilg, H., Zmora, N., Adolph, T.E. & Elinav, E. (2020) The intestinal microbiota fuelling metabolic inflammation. *Nat. Rev. Immunol.*, **20**, 40-54.

Wan, J., Yu, Q., Luo, J., Zhang, L. & Ruan, Z. (2022) Effects of ferulic acid on the growth performance, antioxidant capacity, and intestinal development of piglets with intrauterine growth retardation. *J. Anim. Sci.*, **100**, skac144.

Wang, L., Cao, Z.M., Zhang, L.L., Li, J.M. & Lv, W.L. (2022a) The role of gut microbiota in some liver diseases: from an immunological perspective. *Front. Immunol.*, **13**, 923599.

Wang, X., Yang, F., Na, L., Jia, M., Ishfaq, M., Zhang, Y., Liu, M. & Wu, C. (2022b) Ferulic acid alleviates AFB1-induced duodenal barrier damage in rats via up-regulating tight junction proteins, down-regulating ROCK, competing CYP450 enzyme and activating GST. *Ecotoxicol. Environ. Saf.*, **241**, 113805.

Wang, Y., Xie, Q., Sun, S., Huang, B., Zhang, Y., Xu, Y., Zhang, S. & Xiang, H. (2018) Probiotics-fermented Massa Medicata Fermentata ameliorates weaning stress in piglets related to improving intestinal homeostasis. *Appl. Microbiol. Biotechnol.*, **102**, 10713-10727.

Wang, Y., Zhu, H., Wang, X., Yu, Y. & Xie, J. (2021) Natural food polysaccharides ameliorate inflammatory bowel disease and its mechanisms. *Foods* (*Basel, Switzerland*), **10**, 1288.

Wei, Z., Xue, Y., Xue, Y., Cheng, J., Lv, G., Chu, L., Ma, Z. & Guan, S. (2021) Ferulic acid attenuates non-alcoholic steatohepatitis by reducing oxidative stress and inflammation through inhibition of the ROCK/NF-κB signaling pathways. *J. Pharmacol. Sci.*, **147**, 72-80.

Wu, Y., Zhang, X., Han, D., Ye, H., Tao, S., Pi, Y., Zhao, J., Chen, L. & Wang, J. (2021) Correction to "short administration of combined prebiotics improved microbial colonization, gut barrier, and growth performance of neonatal piglets". *ACS omega*, **6**, 17749.

Xie, Y., Ding, F., Di, W., Lv, Y., Xia, F., Sheng, Y., Yu, J. & Ding, G. (2020) Impact of a high-fat diet on intestinal stem cells and epithelial barrier function in middle-aged female mice. *Mol. Med. Rep.*, **21**, 1133-1144.

Yamamoto, M., Kensler, T.W. & Motohashi, H. (2018) The

KEAP1-NRF2 system: a thiol-based sensor-effector apparatus for maintaining redox homeostasis. *Physiol. Rev.*, **98**, 1169-1203.

Yonezawa, T., Kobayashi, Y. & Obara, Y. (2007) Short-chain fatty acids induce acute phosphorylation of the p38 mitogen-activated protein kinase/heat shock protein 27 pathway via GPR43 in the MCF-7 human breast cancer cell line. *Cell. Signal.*, **19**, 185-193.

Zhao, Z. & Moghadasian, M.H. (2008) Chemistry, natural sources, dietary intake and pharmacokinetic properties of ferulic acid: a review. *Food Chem.*, **109**, 691-702.

Supplementary Files

Please find supplementary file(s);
https://doi.org/10.1620/tjem.2023.J023